International Journal of Technology

http://ijtech.eng.ui.ac.id

Research Article

The Effect of Gas Flow Rate, Solid-To-Solvent Ratio, and Temperature on Micro-Carbon Synthesis from Pine Resin using Spray Pyrolysis and The Application as Masks Coating Material

Jayadi Jayadi [1,2], Wahyu B. Widayatno [2], Agus S. Wismogroho [2], Marga A. J. Mulya [2], Akhiruddin Maddu [1], Yessie W. Sari [1,*]

[1]*Department of Physics, Faculty of Mathematics and Natural Sciences, IPB University, Bogor, 16680, Indonesia*
[2]*National Research and Innovation Agency, Tangerang Selatan, 15310, Indonesia*
[*]*Corresponding author: yessie.sari@apps.ipb.ac.id; Tel: +62 251-8625-728*

Abstract: This study aims to develop an additional layer in masks using micro-carbon to enhance protection against inhalation of droplets. Carbon microstructures were obtained using spray pyrolysis method, with the precursor being resina colophonium dissolved in acetone and ethyl acetate. Subsequently, the effect of varying the precursor-solvent ratio, heating temperature, and nitrogen flow rate on the shape, size, and content of the products was assessed. The results showed that the highest carbon content achieved was approximately 96%, with the smallest size measuring 139 nm. The penetration test results after applying the product on masks fabric revealed a significant reduction in penetration up to level 2. In addition, the contact angle test showed that the addition of carbon led to a lower reduction (6.7°) compared to regular masks fabric with a 20.4° decrease. This improvement could contribute to reducing the risk of droplet inhalation during masks application.

Keywords: Carbon; Mask; Penetration level; *Resina colophonium;* Spray pyrolysis

1. Introduction

Severe acute respiratory syndrome coronavirus 2 (SARS-CoV2) is primarily transmitted through the inhalation of aerosol particles or droplets containing the virus, which are emitted during breathing and speaking (Anfinrud et al., 2020). To reduce the transmission rate, several studies have proposed the use of masks to prevent aerosol particles and droplets from being inhaled. However, the use of these protective materials does not provide absolute protection against the virus (Ueki et al., 2020). This indicates that there is a pressing need to evaluate the effectiveness of masks protection by determining their ability to prevent the entry or exit of droplets (Cheng et al., 2021). The effectiveness of existing masks in the market can be enhanced through the incorporation of an additional layer of carbon (Dizbay-Onat, 2023) obtained from coconut shells (Sujiono et al., 2022), palm oil shells (Rashidi and Yusup, 2019), or wood (Efiyanti et al., 2023). This added layer is typically added to trap the virus by adsorbing moisture. After the virus is captured, highly electropositive ions can disrupt the integrity of the membrane and vital proteins, degrading the ability to function (Reza et al., 2021).

This work was supported by the National Research and Innovation Agency funded by DIPA of Research Organization of Nanotechnology and Materials with contract number of B-392/III/HK.01.00/2/2022

https://doi.org/10.14716/ijtech.v16i3.6252
Received December 2022; Revised May 2023; Accepted September 2023

According to previous studies, carbon-based precursor materials are traditionally synthesized using a solution of methanol (Fang et al., 2018), benzene (Melati and Hidayati, 2016), xylene (Singhal et al., 2019), or toluene (Khabushev et al., 2022) derived from fossil fuels. However, the limited nature of these resources (Sulistya et al., 2020) necessitates the exploration of alternatives to produce nanostructured carbon, such as cellulose (Harahap et al., 2023), biomass (Politaeva et al., 2020), and turpentine oil (Suhas et al., 2016). In this context, turpentine oil, derived from the distillation of pine resin (*resina colophonium)* serves as a promising alternative. *Resina colophonium* is widely used as a raw material for producing resins or solvents for paint mixtures (Rucitra and Amna, 2021). In 2018, a total of 92,550 tons of *resina colophonium* was produced by 8 companies in Indonesia (Afre et al., 2006), contributing to the global production of approximately 1.3 million tonnes (Song, 2019). Various methods, including hydrothermal, templates, physical/chemical vapor deposition (Papaioannou et al., 2018), and spray pyrolysis (Vishwanathan et al., 2018) have been proposed for the synthesis of carbon-based precursor materials. Among these methods, spray pyrolysis is considered the most common and it comprises the decomposition of precursor molecules at high temperatures. In addition, the decomposition process is often carried out using spray pyrolysis instrument system, comprising a precursor atomizer, carrier gas flow, heating reactor, and carbon collector media (Jayadi et al., 2024). Atomized precursor molecules, facilitated by gas flow (nitrogen/argon), are transferred to the heating reactor, where breakdown occurs. The molecules are broken down to produce carbon granules, which are then captured in the collector media (Park et al., 2019).

In line with these results, Liu et al. conducted a study on the ultrasonic spray pyrolysis method for synthesizing nitrogen-doping carbon nanotubes. The procedures were carried out at injection rates of 0.25, 0.5, and 0.75 ml/minute, while the gas flow rate at each inlet was maintained at 150 sccm (Liu et al., 2011). Ionescu et al. (2011) also explored the synthesis of nanotubes from ferrocene and xylene precursors using the same method with argon as carrier gas at a flow rate of 175 sccm and temperature at 700-800°C (Ionescu et al., 2011). In addition, a similar process was performed by Yan et al using chopped pine trees with nitrogen flow under atmosphere pressure at different temperatures. Each temperature run was carried out at 500 mL/minute gas flow rate, 10°C/minute heating rate, and 30 minutes pyrolysis time. The results showed that increasing the flow velocity of argon gas during the synthesis process had a significant impact (Yan et al., 2011). Therefore, this study aims to develop an additional layer in masks using micro-carbon from pine resin precursor (*resina colophonium)* synthesized with spray pyrolysis method. The synthesis process was carried out using varying parameters, such as precursor composition (*resina colophonium:* solvent), temperature, and carrier gas flow rate to determine their effects. FE-SEM EDS test was used to determine the sample morphology, particle size, and carbon content. Meanwhile, functional assessment of additional layer of masks was carried out using penetration and contact angle tests.

2. Materials and Methods

2.1. Materials

Pine resin (*resina colophonium*), which was essential for the experiments, was obtained from the local market. The solvents used were acetone (pro analysis 99.75%, Mallinckrodt Chemicals) and ethyl acetate (pro analysis 99.8%, Merck KGaA).

2.2. Micro-Carbon Preparation

Micro-carbon materials, which were crucial for the study, were obtained through spray pyrolysis of pine resin. In this process, pine resin was dissolved in either acetone (GAC) or ethyl acetate (GEA). Pine resin was firstly crushed by a Hamer mill (5000 rpm German) until it reached a size of 60 mesh to facilitate the dissolving process.

The in-house spray pyrolysis was utilized for the experiment. This instrument was configured to allow the precursor (GAC or GEA) into the inlet, atomized, and subsequently conveyed into a heating reactor with the aid of nitrogen gas. During the heating process, pine resin underwent

decomposition, which yielded carbon granules that were deposited onto a 1000-wire mesh positioned at the outlet of the heating reactor. Spray pyrolysis was set for 20 minutes for each variation. This study involved varying the ratio of pine resin to solvent and adjusting the nitrogen gas flow rate during micro-carbon synthesis. Specifically, the ratios of pine resin to solvent were set at 1:4, 1:8, and 1:16 (g/ml). The heating temperature was varied at 800, 1000, and 1200°C, while the nitrogen gas flow rates were adjusted to 0.5, 1, and 1.5 liter/minute. These parameters were selected to achieve the highest percentage of carbon content while maintaining a smooth carbon surface to repel droplets.

2.3. Application of Micro-Carbon as Mask Layer

Polypropylene sheet, which was a common medical mask, (80 x 80 cm), was used as masks. Micro-carbon was deposited on this sheet using vacuum chambers with a volume of 1 liter (VC1621SG, VacuumChambers.ue., Poland).

Before deposition, the product was first dissolved in acetone with a ratio of 0.3 g/ml. The dissolved micro-carbon was placed in the vacuum chamber at around 25 ± 2°C and under a pressure of 50 kPa for 30 minutes. Micro-carbon coated masks were further dried using the conventional oven at 60°C for 24 hours (Aristri et al., 2021). The amount of micro-carbon was calculated as the difference in masks mass before and after deposition.

2.4. Sample Characterization

2.4.1. Morphological Analysis

The synthesized micro-carbon powder was separated from the surface of wire mesh 1000 for morphological analysis using Field Emission Scanning Electron Microscopy (FESEM, JIB-4610F, Jeol Ltd Japan). Images obtained from FESEM were further analyzed using ImageJ to obtain the average particle size. As many as 20 particles were evaluated to obtain this parameter, FESEM analysis was also combined with energy-dispersive X-ray spectroscopy to evaluate the carbon content.

2.4.2. Penetration Test

Penetration test was performed according to ISO 16603:2004 about measuring the penetration resistance of clothing materials to blood and body fluids. There were 6 pressure levels involved in this test (Table 1), and to imitate saliva penetration on a surface, chicken egg white was utilized as it was considered to have a surface tension close to saliva. The surface tension of egg white without yolk contamination was 50 mN/m (Li et al., 2022), yolk only was 44 mN/m (Miranda et al., 2022), while human saliva was about 58 mN/m (Gittings et al., 2015).

The penetration test was conducted by applying varying pressure levels after egg white was applied to the test samples. The test was terminated once egg white penetrated through the test sample. When penetration did not occur, the test proceeded to the next level by increasing the pressure. Table 2 listed samples involved in this study.

Table 1 Test level in penetration test and waiting time for each level

Level	Pressure (kPa)	Time (Minutes)
1	0	5
2	1.75	
3	3.5	
4	7	
5	14	
6	20	

2.4.3. Contact Angle Test

Assessing the absorption property of masks coated with micro-carbon involved conducting contact angle test on the samples. This test entailed dropping a liquid onto the test samples, capturing an image of the sample, and observing the angle formed between the liquid and the

sample (Whulanza et al., 2020). Angle was measured by manually drawing lines along the edge of the liquid-sample boundary in the captured picture, and the corresponding angular values were automatically calculated using DinoCapture 2.0 software. When the dropped liquid was absorbed by the test sample, the angle decreased. The contact angle data were recorded every 10 minutes for a total of 1 hour of observation. Masks sheets coated with GAC or GEA micro-carbon having relatively equal carbon weight were selected for this test. Observation of contact angle was conducted using a digital microscope Dino-Lite Plus with the ability to magnify 20-90 times.

Table 2 Sheet samples code used

Code	Sample
PS sample	polypropylene sheet without any coating
PAC sheet	commercial polypropylene sheet coated with activated carbon
GAC sheet	polypropylene sheet coated with carbon dissolved in GAC
GEA sheet	polypropylene sheet coated with carbon dissolved in GEA

3. Results and Discussion

3.1. Micro-Carbon Synthesis: Effect of Solid-To-Solvent Ratio

The morphologies of micro-carbon resulting from pyrolysis at 1000°C with various solid-to-solvent ratios (1:4, 1:8, and 1:16) were shown in Figure 1. FESEM results indicated that micro-carbon particles had round and smooth surfaces. In this test, the value of carbon content in the sample could also be known. As shown in Table 3, all samples were rich in carbon content with a value of more than 90%. The highest carbon content was obtained in samples from GAC precursors with a composition ratio of 1:8, which reached 96.8% wt.

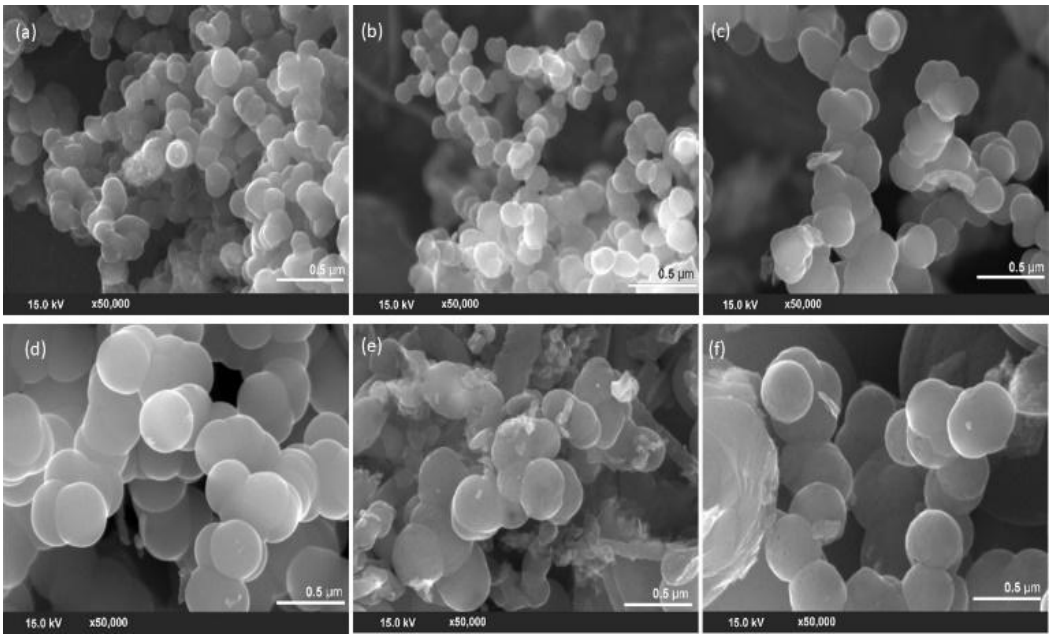

Figure 1 FESEM images of micro-carbon particles size obtained with pine resin solvent ratio of (a) 1:4 (b) 1:8 (c) 1:16 from GAC samples and (d) 1:4 (e) 1:8 (f) 1:16 from GEA samples

Particle size could be determined quantitatively based on the measuring scale performed on FE-SEM test results. Micro-carbon of GAC samples had a smaller particle size than micro-carbon from GEA samples (Figure 2). Micro-carbon from precursor GAC with pine resin to acetone ratio of 1:8 had the smallest average particle size, which was 0.12 µm. Figure 2 showed the normal distribution, the average value (µ), and the standard deviation (σ) of all samples. The distribution of carbon diameter of GAC samples indicated less distribution compared to GEA counterpart. This could be

due to the agglomeration of crushed pine resin in ethyl acetate. Previous studies indicated that agglomeration in ethyl acetate was quicker to form rather than in ethanol (Shukla et al., 2017). This agglomeration could also lead to inhomogeneity of particle size as seen in Figure 1. e.

Table 3 Carbon content in samples with pine resin to solvent ratio

Sample	Pine resin to solvent ratio	Relative carbon content (% wt)
GAC	1:4	95.625
	1:8	96.862
	1:16	96.525
GEA	1:4	96.275
	1:8	96.037
	1:16	96.337

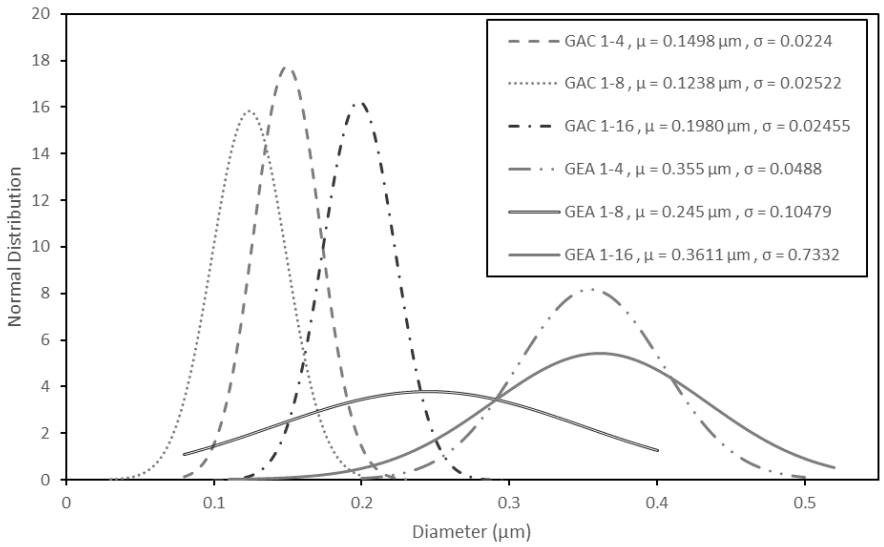

Figure 2 Particle size distribution of GAC and GEA from 20 particles of each sample

3.2. Micro-Carbon Synthesis: Effect of Pyrolysis Temperature

Figure 3, the measurement scale of FE-SEM test resulting from carbon samples synthesized at various heating temperatures with GAC at pine resin to solvent ratio of 1:16 and a nitrogen gas flow rate of 1 liter/minute. Additionally, it was observed that synthesis at 800°C resulted in micro-carbon with the lowest particle size, 0124 ± 0.008 μm. However, the particle sizes in these samples were observed to have a heterogeneous morphology. An improved morphology heterogeneity was observed at micro-carbon obtained from pyrolysis at 1000 and 1200°C (Figures 3b and c, respectively). Micro-carbon synthesized at 1200°C had the highest particle size homogeneity, and the particle surface had an imperfection. Figure 3c showed that the surface of these particles was not smooth, and the distribution of particle size was obtained from various pyrolysis temperatures.

Pyrolysis temperature also influenced the content of the resulting carbon, and the sample at a synthesis temperature of 1000°C had the highest carbon content, reaching 96.5% wt (Table 4). The increase in carbon content at 1000°C and 1200°C compared to 800°c reflected the increasing degree of carbonization (Chatterjee et al., 2020). With the objective of achieving micro-carbon with high carbon content, masks coating was therefore conducted with micro-carbon synthesized at 1000°C.

3.3. Micro-Carbon Synthesis: Effect of Nitrogen Flow

Table 5 showed that samples synthesized at 1200°C had similar carbon content to the sample at 1000°C but had bigger particle sizes (Figure 6) and rougher surfaces (Figure 5). Exploring whether adjusting the nitrogen gas flow rate could improve either carbon content, particle size, or surface

characteristics, the nitrogen flow rate variation test was conducted on GAC 1:16 sample heated at 1200°C.

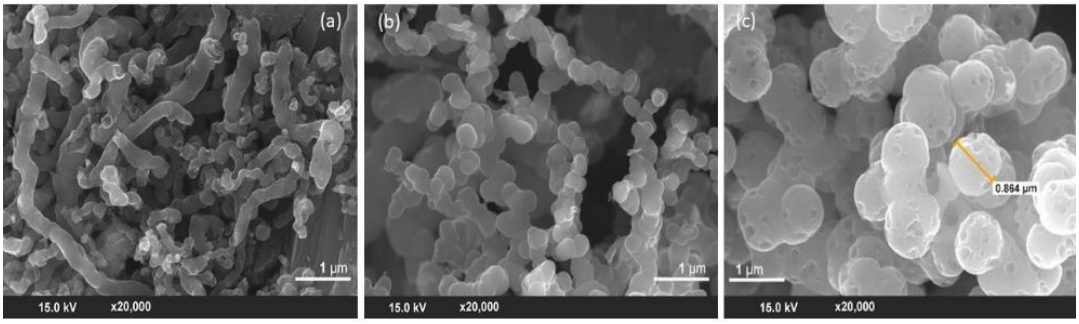

Figure 3 FESEM images of GAC samples obtained from pine resin, a solvent ratio of 1:16, nitrogen gas flow rate of 1 liter/minute, and synthesis temperature, (a) 800°C, (b) 1000°C, and (c) 1200°C

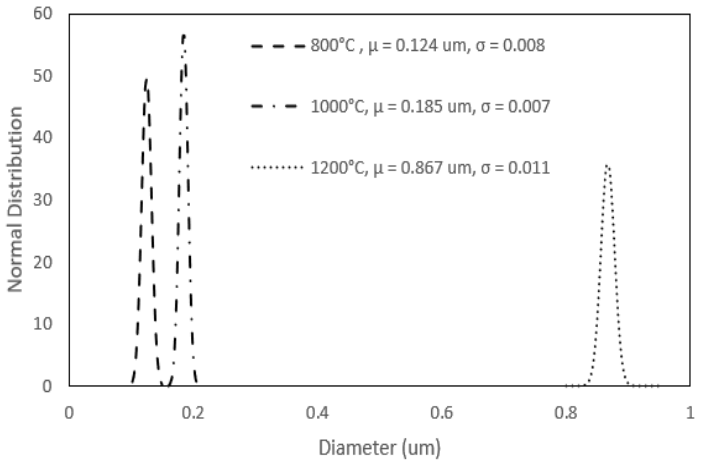

Figure 4 Particle size distribution of GAC precursor 1:16 with nitrogen gas flow rate of 1 liter/minute at a varied synthesis temperature

Table 4 Carbon content in samples of GAC 1:16 precursors with variations in synthesis temperature

Synthesis temperature (°C)	Relative carbon content (% wt)
800	92.475
1000	96.525
1200	96.275

Based on the image processing of FESEM images, the smallest particle size was formed at a flow rate of 0.5 liter/minute, which was 0.167 ± 0.008 µm. All carbon materials were synthesized at a pyrolysis temperature of 1200°C with varied nitrogen flow rates showing rough surfaces as shown in Figure 5.

Table 5 Carbon content in samples from GAC 1:16 precursors with a synthesis temperature of 1200°C and variations in nitrogen flow rate

Nitrogen flow rate (liter/ minute)	Relative carbon content (at%)
0.5	14.48
1	96.28
1.5	97.15

An interesting observation was made regarding the significant influence of nitrogen flow rate on the carbon content of the samples. As shown in Table 5, at a nitrogen flow rate of 0.5 l/minute,

micro-carbon with a content of 14.48% wt was obtained, suggesting the presence of volatiles that acted as catalysts for secondary reactions, potentially reducing carbon yield (Wang et al, 2021; Sukumar et al., 2020). With an increase in the nitrogen flow rate, the carbon content substantially increased, reaching 96.28% by weight when doubled and 97.15% by weight when tripled.

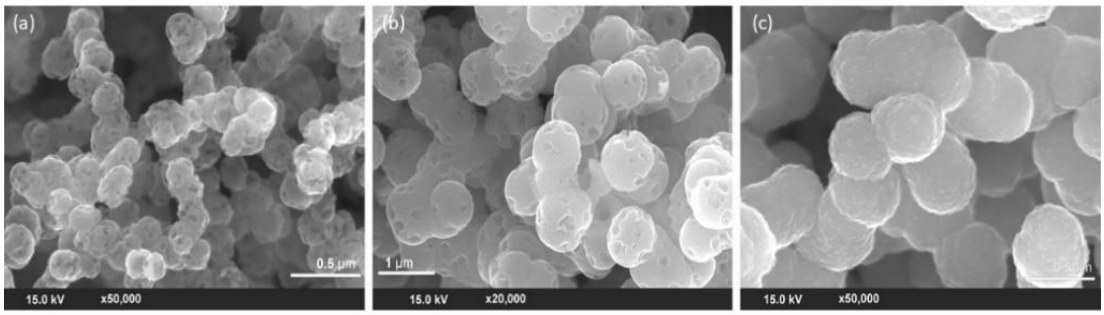

Figure 5 Carbon particle size of GAC precursor 1:16 with synthesis temperature 1200°C and nitrogen gas flow rate (a) 0.5 liter/minute (b) 1 liter/minute (c) 1.5 liter/minute

3.4. Application of Micro-Carbon as Masks Layer

Both GAC and GEA micro-carbon obtained at pine resin to solvent ratio of 1:8, 1000°C pyrolysis temperature, and 1 liter/minute of nitrogen flow rate were tested for their application as masks coating materials. The selection was based on the data discussed in sections 3.1, 3.2, and 3.3, indicating that at this condition, the product had the smallest particle size, the smoothest surface, and the highest carbon content. The small particle size was preferred as micro-carbon particles were expected to be able to close the gap in polypropylene sheet.

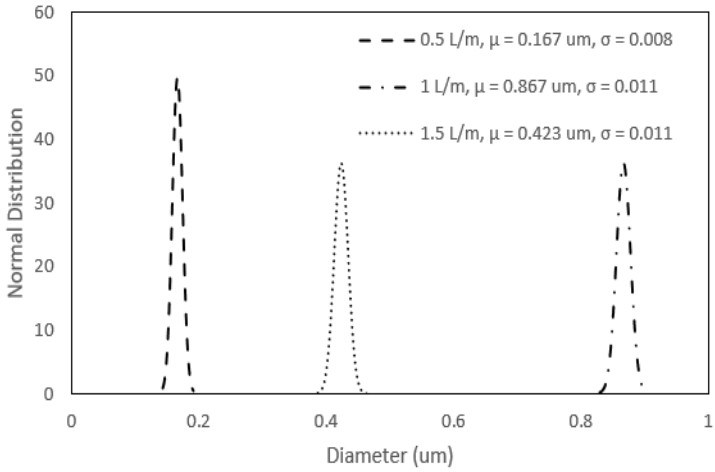

Figure 6 Particle size distribution of GAC precursor 1:16 with synthesis temperature 1200°C and varied nitrogen gas flow rate

Figures 7 a, b, c, and d showed the dropped water on polypropylene sheet coated with the product, and the yellow line on these figures indicated the contact angle. Observations were conducted for 1 hour and contact angle data were recorded every 10 minutes. Table 6 indicated the data from the contact angle observations. Based on the data in Figure 8a, all samples had initial contact angles above 90°, indicating that all paper masks were hydrophobic (Yuan and Lee, 2013).

The contact angle was observed to decrease along with the observation time. Comparison between all samples in this test at minute 0 and minute 60 could be seen in Figure 8b. A significant decrease was experienced by PS sample, from an initial contact angle of 118.221° to 97.802° (20.4° difference). The least decrease in contact angle was experienced in GAC sheet from 121.530° to 114.744° (6.786° difference). This indicated that the presence of a carbon layer on polypropylene sheet could reduce or slow down the absorption process. GEA sheet had less performance in this

test (10.8° drop from 120.4°) compared to GAC sheet. This result designated that the difference in size affected the results of this test. PAC sheet, which was polypropylene coated with commercial activated carbon, had a higher contact angle drop from 118.852° to 101.162° (17.69° difference) compared to polypropylene coated with GAC and GEA micro-carbon. Activated carbon was generally used as an adsorbent which relied on the porous surface (Politaeva et al., 2020). Water or saliva could readily permeate through the pores on activated carbon compared to GAC and GEA sheets, which had a smoother surface. This property allowed to seal gaps in masks cloth which made it challenging for liquid to pass through. After several experiment repetitions, the measurement data did not deviate much as depicted in Figure 8b.

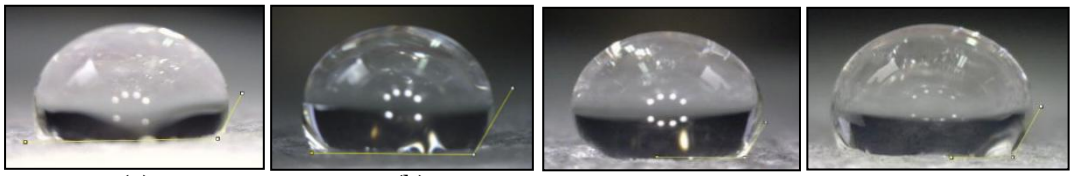

Figure 7 Initial contact angle for (a) PS sample, (b) PAC sheet, (c) GEA sheet, (d) GAC sheet

In Table 6, presented below, the result of the penetration test showed that both PS sample and PAC sheet were effectively penetrated by egg white at level 1 or without any pressure applied. Activated carbon coated on polypropylene sheet proved unable to withstand the penetration of egg white in the test. This could occur because the pores in the activated carbon could serve as a pathway for egg white to penetrate the sheet.

Table 6 Penetration test results for all samples and carbon weight applied

Test Sample	Carbon weight (g)	Penetration level	Pressure (kPa)
PS sample	-	Level 1	0
PAC sheet	n.d	Level 1	0
GAC sheet	0.0043	Level 1	0
	0.0150	Level 1	0
	0.0167	Level 2	1.75
GEA sheet	0.0044	Level 1	0
	0.0166	Level 2	1.75
	0.0206	Level 3	3.5

n.d, not determined

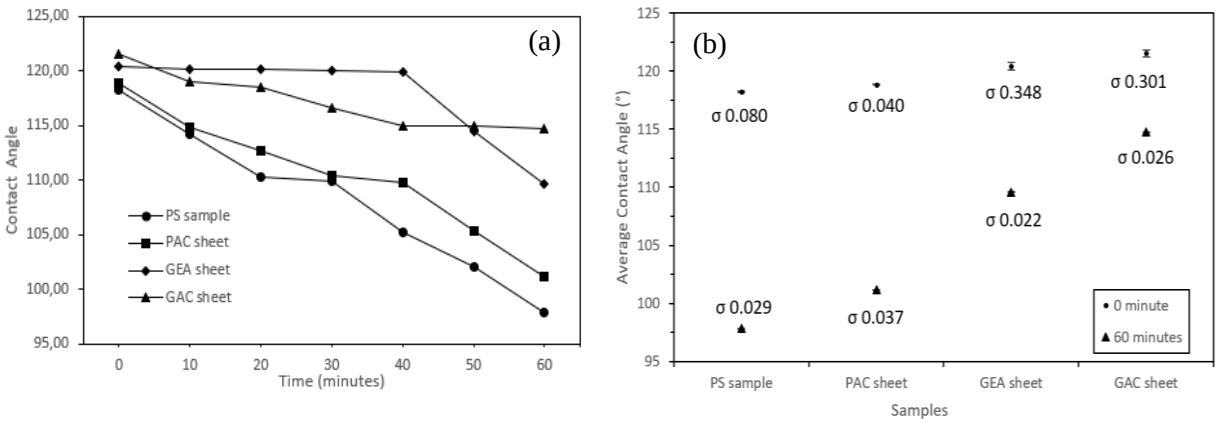

Figure 8 Contact angle test data (a) taken every 10 minutes for 1 hour, (b) test data distribution after 20 measurements at minutes 0 and 60

Penetration was also experienced by both GAC and GEA sheets. However, it was observed that a pressure of min 1.75 kPa was required to let egg white penetrate these sheets. This result showed the potential of micro-carbon synthesized from pine resin as masks coating materials. At GEA sheet, it was observed that an increase in the mass of the product resulted in an increase in required pressure for the egg white penetration. This indicated that the amount of micro-carbon had an effect on masks adsorption properties. Therefore, further studies were needed to evaluate the optimum micro-carbon mass required for the optimum adsorption.

4. Conclusions

In conclusion, the study analysis indicated that micro-carbon was successfully synthesized using a mixture of resina colophonium mixed with acetone and ethyl acetate as solvents. The precursor composition, synthesis temperature, and nitrogen flow rate played significant roles in shaping the size, and carbon content during spray pyrolysis method. Specifically, a 1:8 ratio of resina colophonium to acetone resulted in particles measuring 139 nm with a carbon content of 96.682%, while the same ratio with ethyl acetate produced larger particles (301 nm) with a slightly lower content of 96.037%. Furthermore, coating polypropylene sheets with the product led to improved performance. This was evidenced by superior contact angle and penetration test results compared to non-coated and commercially coated sheets. The addition of micro-carbon effectively reduced the risk of droplet inhalation.

Acknowledgements

The authors are grateful to the National Research and Innovation Agency for the facilities and funding provided with contract number B-392/III/HK.01.00/2/2022.

Author Contributions

All authors contributed to the study conception and design. Material preparation and data collection were performed by **Jayadi, Wahyu B. Widayatno and Agus S. Wismogroho**. The first draft of the manuscript was written by **Jayadi and Marga A. J. Mulya**. **Akhiruddin Maddu and Yessie W. Sari** carried out thorough data analysis and interpretation. All authors commented on previous versions of the manuscript.

Conflict of Interest

The authors declare that they have no known competing financial interests or personal relationships that could have appeared to influence the work reported in this paper.

References

Afre, RA, Soga, T, Jimbo, T, Kumar, M, Ando, Y, Sharon, M, Somani, PR & Umeno, M 2006, 'Carbon nanotubes by spray pyrolysis of turpentine oil at different temperatures and their studies', *Microporous and Mesoporous Materials*, vol. 96, no. 1–3, pp. 184–190, https://doi.org/10.1016/j.micromeso.2006.06.036

Anfinrud, P, Stadnytskyi, V, Bax, CE & Bax, A 2020, 'Visualizing speech-generated oral fluid droplets with laser light scattering', *New England Journal of Medicine*, vol. 382, no. 21, pp. 2061–2063, https://doi.org/10.1056/NEJMc1913036

Aristri, MA, Lubis, MAR, Laksana, RPB, Falah, F, Fatriasari, W, Ismayati, M, Wulandari, AP, Nurindah, N & Ridho, MR 2021, 'Bio-polyurethane resins derived from liquid fractions of lignin for the modification of ramie fibers', *Jurnal Sylva Lestari*, vol. 9, no. 2, article 223, http://dx.doi.org/10.23960/jsl29223-238

Chatterjee, R, Sajjadi, B, Chen, WY, Mattern, DL, Hammer, N, Raman, V & Dorris, A 2020, 'Effect of pyrolysis temperature on physicochemical properties and acoustic-based amination of biochar for efficient CO_2 adsorption', *Frontiers in Energy Research*, vol. 8, article 85, https://doi.org/10.3389/fenrg.2020.00085

Cheng, Y, Ma, N, Witt, C, Rapp, S & Wild, PS, Andreae, MO, Pöschl, U, & Su, H 2021, 'Face masks effectively limit the probability of SARS-CoV-2 transmission', *Science*, vol. 372, no. 6549, pp. 1439–1443, https://doi.org/10.1126/science.abg6296

Dizbay-Onat, M 2023, 'Evaluation of physical adsorption properties of the activated carbon layers used in the commercial face mask inserts', *Eng*, vol. 4, no. 1, pp. 434–443, https://doi.org/10.3390/eng4010026

Efiyanti, L, Rifa'i, FA, Maslahat, M, Indrawan, DA, Wibowo, S, Darmawan, S, Pari, R, Pasaribu, G, Rahmila, YI, Agustarini, R, Aswandi, A, Kholibrina, CR, Santoso, A, Djarwanto, Komarayati, S, Gusmalina, Pari, G & Hendra, D 2023, 'CO/activated carbon from Paraserianthes falcataria as a green catalysts for plastic waste pyrolysis', *RASAYAN Journal of Chemistry*, vol. 16, no. 3, pp. 1149–1162, https://doi.org/10.31788/RJC.2023.1638347

Fang, R, Huang, H, Ji, J, He, M, Feng, Q, Zhan, Y & Leung, DY 2018, 'Efficient MnOx supported on coconut shell activated carbon for catalytic oxidation of indoor formaldehyde at room temperature', *Chemical Engineering Journal*, vol. 334, pp. 2050–2057, https://doi.org/10.1016/j.cej.2017.11.176

Gittings, S, Turnbull, N, Henry, B, Roberts, CJ & Gershkovich, P 2015, 'Characterisation of human saliva as a platform for oral dissolution medium development', *European Journal of Pharmaceutics and Biopharmaceutics*, vol. 91, pp. 16–24, https://doi.org/10.1016/j.ejpb.2015.01.007

Harahap, M, Daulay, N, Zebua, D & Gea, S 2023, 'Nanofiber cellulose/lignin from oil palm empty fruit bunches and the potential for carbon fiber precursor prepared by wet-spinning', *International Journal of Technology*, vol. 14, no. 1, pp. 152–161, https://doi.org/10.14716/ijtech.v14i1.5082

Ionescu, MI, Zhang, Y, Li, R, Sun, X, Abou-Rachid, H, & Lussier, LS 2011, 'Hydrogen-free spray pyrolysis chemical vapor deposition method for the carbon nanotube growth: Parametric studies', *Applied Surface Science*, vol. 257, no. 15, pp. 6843–6849, https://doi.org/10.1016/j.apsusc.2011.03.011

Jayadi, Widayatno WB, Wismogroho AS, Firdharin C, Maddu, A, Alatas, H & Sari, YW 2024, 'Effect of precursor solvent on the carbon micro-structures derived from spray pyrolysis of pine resin (gondorukem): Preliminary study', *Jurnal Sains Materi Indonesia*, vol. 25, no. 2, pp. 67–76, https://doi.org/10.55981/jsmi.2024.893

Khabushev, EM, Krasnikov, DV, Goldt, AE, Fedorovskaya, EO, Tsapenko, AP, Zhang, Q, Kauppinen, EI, Kallio, T & Nasibulin, AG 2022, 'Joint effect of ethylene and toluene on carbon nanotube growth', *Carbon*, vol. 189, pp. 474–483, https://doi.org/10.1016/j.carbon.2021.12.052

Li, X, Wang, Y, Lv, J & Yang, Y 2022, 'Investigations of foaming, interfacial and structural properties of dispersions, batters and cakes formed by industrial yolk-contaminated egg white protein', *LWT*, vol. 154, pp. 1–9, https://doi.org/10.1016/j.lwt.2021.112776

Liu, J, Zhang, Y, Ionescu, MI, Li, R & Sun, X, 2011, 'Nitrogen-doped carbon nanotubes with tunable structure and high yield produced by ultrasonic spray pyrolysis', *Applied Surface Science*, vol. 257, no. 17, pp. 7837–7844, https://doi.org/10.1016/j.apsusc.2011.04.041

Melati, A, & Hidayati, E 2016, 'Synthesis and characterization of carbon nanotube from coconut shells activated carbon', *Journal of Physics: Conference Series*, vol. 694, article 012073, https://doi.org/10.1088/1742-6596/694/1/012073

Miranda, J, Partal, P, Cordobés, F & Guerrero, A, 2002, 'Rheological characterization of egg yolk processed by spray-drying and lipid-cholesterol extraction with carbon dioxide', *Journal of the American Oil Chemists Society,* vol. 79, no. 2, pp. 183-190

Papaioannou, N, Marinovic, A, Yoshizawa, N, Goode, AE, Fay, M, Khlobystov, A, Titirici, MM & Sapelkin, A 2018, 'Structure and solvents effects on the optical properties of sugar-derived carbon nanodots', *Scientific Reports*, vol. 8, no. 1, article 6559, https://doi.org/10.1038/s41598-018-25012-8

Park, J-S, Kim, JK, Hong, JH, Cho, JS, Park, S-K & Kang, YC 2019, 'Advances in the synthesis and design of nanostructured materials by aerosol spray processes for efficient energy storage', *Nanoscale*, vol. 11, no. 41, pp. 19012–19057, https://doi.org/10.1039/C9NR05575D

Politaeva, N, Taranovskaya, E, Mukhametova, L, Ilyashenko, S, Atamanyuk, I, Al Afif, R, & Pfeifer, C 2020, 'Cotton fiber and carbon materials filters for efficient wastewater purification', *International Journal of Technology*, vol. 11, no. 8, pp. 1608-1617, https://doi.org/10.14716/ijtech.v11i8.4538

Rashidi, NA, & Yusup, S 2019, 'Production of palm kernel shell-based activated carbon by direct physical activation for carbon dioxide adsorption', *Environmental Science and Pollution Research*, vol. 26, no. 33, pp. 33732–33746, https://doi.org/10.1007/s11356-018-1903-8

Reza, MS, Hasan, ABMK, Ahmed, AS, Afroze, S, Bakar, MSA, Islam, SN & Azad, AK 2021, 'COVID-19 prevention: Role of activated carbon', *Journal of Engineering and Technological Sciences*, vol. 53, no. 4, pp. 628–638, https://doi.org/10.5614/j.eng.technol.sci.2021.53.4.4

Rucitra, AL & Amna, AUF 2021, 'Integration of statistical quality control (SQC) and fault tree analysis (FTA) in the quality control of resina colophonium production in company X', *In:* IOP Conference Series: Earth and Environmental Science, vol. 924, no. 1, article 012062, https://doi.org/10.1088/1755-1315/924/1/012062

Shukla, S, Bhattacharjee, S, Weber, AZ & Secanell, M 2017, 'Experimental and theoretical analysis of ink dispersion stability for polymer electrolyte fuel cell applications', *Journal of The Electrochemical Society*, vol. 164, no. 6, pp. F600–F609, https://doi.org/10.1149/2.0961706jes

Singhal, S, Dixit, S & Shukla, AK 2019, 'Structural analysis of carbon nanospheres synthesized by CVD: An investigation of surface charges and its effect on the stability of carbon nanostructures', *Applied Physics A*, vol. 125, article 80, https://doi.org/10.1007/s00339-018-2372-0

Song, L 2019, *The overview of today's pine chemical industry in China*, Pine Chemicals Association, Vancouver

Suhas, Gupta, VK, Carrott, PJM, Singh, R, Chaudhary, M & Kushwaha, S 2016, 'Cellulose: A review as natural, modified and activated carbon adsorbent', *Bioresource Technology*, vol. 216, pp. 1066–1076, https://doi.org/10.1016/j.biortech.2016.05.106

Sujiono, EH, Zabrian, D, Zharvan, V & Humairah, NA 2022, 'Fabrication and characterization of coconut shell activated carbon using variation chemical activation for wastewater treatment application', *Results in Chemistry*, vol. 4, article 100291, https://doi.org/10.1016/j.rechem.2022.100291

Sukumar, V, Manieniyan, V, Senthilkumar, R & Sivaprakasam, S 2020, 'Production of bio oil from sweet lime empty fruit bunch by pyrolysis', *Renewable Energy*, vol. 146, pp. 309–315, https://doi.org/10.1016/j.renene.2019.06.156

Sulistya, EH, Hui-Hui, L, Attenborough, NK, Pourshahrestani, S, Kadri, NA, Zeimaran, E, Razak, NAbA, Horri, BA & Salamatinia, B 2020, 'Hydrothermal synthesis of carbon microspheres from sucrose with citric acid as a catalyst: Physicochemical and structural properties', *Journal of Taibah University for Science*, vol. 14, no. 1, pp. 1042–1050, https://doi.org/10.1080/16583655.2020.1794566

Ueki, H, Furusawa, Y, Iwatsuki-Horimoto, K, Imai, M, Kabata, H, Nishimura, H & Kawaoka, Y, 2020, 'Effectiveness of face masks in preventing airborne transmission of SARS-CoV-2', *mSphere*, vol. 5, no. 5, article e00637-20, https://doi.org/10.1128/msphere.00637-20

Vishwanathan, LG, Bhowmik, S & Sharon, M 2018, 'Natural precursors for synthesis of carbon nano materials by chemical vapor deposition process: A review', *International Journal of Science and Research*, vol. 7, no. 2, pp. 1475–1485, https://doi.org/10.21275/ART2018338

Wang, M, Wang, Q, Li, T, Kong, J, Shen, Y., Chang, L, Xie, W & Bao, W, 2021, 'Catalytic upgrading of coal pyrolysis volatiles by porous carbon materials derived from the blend of biochar and coal', *ACS Omega,* vol. 6, no. 5, pp. 3800–3808

Whulanza, Y, Supriadi, S, Chalid, M, Kreshanti, P, Agus, AA, Napitupulu, P, Supriyanto, JW, Rivai, E & Purnomo, A 2020, 'Setting acceptance criteria for a national flocked swab for biological specimens during the COVID-19 pandemic', *International Journal of Technology*, vol. 11, no. 5, pp. 888–899, https://doi.org/10.14716/ijtech.v11i5.4335

Yan, Q, Toghiani, H, Yu, F, Cai, Z & Zhang, J 2011, 'Effects of pyrolysis conditions on yield of bio-chars from pine chips', *Forest Products Journal*, vol. 61, no. 5, pp. 367–371, https://www.doi.org/10.13073/0015-7473-61.5.367

Yuan, Y & Lee, TR, 2013, 'Contact angle and wetting properties', *Springer Series in Surface Sciences*, vol. 51, no. 1, pp. 3–34, https://doi.org/10.1007/978-3-642-34243-1_1